Anal. Bioanal. Electrochem., Vol. 16, No. 10, 2024, 910-927
https://www.doi.org/10.22034/abec.2024.717549

Analytical & Bioanalytical Electrochemistry

www.abechem.com

Full Paper

Simultaneous Determination of *p*-Benzoquinone and Resorcinol at Reduced Graphene Oxide Modified Glassy Carbon Electrode

Eleilde de S. Oliveira,* Aldaléa L. B. Marques,* Ismael Carlos B. Alves, Edmar P. Marques, José Ribamar N. dos Santos, Raquel B. dos S. Sawczuk, Lorena C. Martiniano de Azevedo, and Janyeid Karla Castro Sousa

Nucleus for Studies in Petroleum and Energy (NEPE): LPQA & LAPQAP, Department of Chemical Technology, Federal University of Maranhão (UFMA), São Luís - MA, Brazil

*Corresponding Author, Tel.: +55-98982499364

E-mails: aldalea.brandes@ufma.br ; eleildeoliver@gmail.com

Received: 19 June 2024 / Received in revised form: 18 October 2024 / Accepted: 24 October 2024 / Published online: 31 October 2024

Abstract- In this work we report the development of an electrochemical sensor based on a modified glassy carbon electrode (GCE) modified with reduced graphene oxide (rGO) for simultaneous determination of *p*-benzoquinone (BQ) and resorcinol (RS) in soil and water samples of gas stations, using the electrochemical techniques of cyclic voltammetry (CV), electrochemical impedance spectroscopy (EIS), and square wave voltammetry (SWV). The sensor modification was carried out by drop casting, a 10 µL aliquot of the rGO suspension was dropped onto the surface of the GCE. The sensor showed a linear response for both analytes through SWV from 20 µM up to 100 µM. Good results of sensitivity, limit of detection (LOD), and quantification (LOQ) were obtained for BQ (0.03 µA μM^{-1}, 0.37 µM, and 1.23 µM) and RS (0.07 µA μM^{-1}, 0.81 µM, and 2.71 µM), respectively. The method was tested in environmental samples (soil and water) through spike and recovery procedure (recovery > 99%), with precision (RSD) of 0.10% (BQ) and 0.36% (RS).

Keywords- Benzene derivatives; Environmental samples; Reduced graphene oxide; Electrochemical determination; Voltammetry

---

1. INTRODUCTION

Contamination of water, soil, and air occurs largely due to the petroleum derivatives. The current transportation infrastructure system will continue to depend for a long time on petroleum products (e.g., gasoline, kerosene, mineral oil, fuel oil, and asphalt), whose environmental contaminants are widespread, harmful, and growing [1].

Among the hydrocarbons present in petroleum oil, BTEX (benzene, toluene, ethylbenzene, and xylenes) are the environmental contaminants that have aroused the most interest in terms of attention, for researchers and environmental agencies [2,3]. These compounds are recognized as potential contaminants in the environment [4,5] and represent a public health problem [5–7]. Environmental contamination occurs mainly due to leaks, spills, and accidents during exploration, refining, transportation, and fuel storage, and distribution operations [4,8].

1,4-benzoquinone or *p*-benzoquinone (BQ) is one of the most abundant, volatile, and reactive quinones [9]. It can be formed by the oxidative process of different benzene derivatives [10,11], becoming a dangerous intermediate, more toxic than phenol [11,12]. Benzene-1,3-diol, also known as resorcinol (RS), is a toxic compound belonging to the phenol class. It has wide industrial applications as a solvent and is present in effluents from various industries, such as petrochemicals, rubber, paper, and cellulose. Furthermore, it is used in the production of cosmetics, antioxidants, and dyes [4,13–15]. Both compounds are common in fuel residues such as diesel oil and gasoline and cause soil and natural water contamination, mainly in regions close to retail fuel stations. Therefore, environmental monitoring of these analytes is necessary.

Considerable interest has been devoted to the development of effective methodology and reliable approaches for the determination of these toxic substances. Several analytical methods are described for the analysis of benzene derivatives, such as liquid chromatography [16], fluorescence [17], chemiluminescence [18], spectrophotometry [19], flow injection chemiluminescence [20], gas chromatography [21], mass spectrometry [22], capillary electrochromatography [23], and electrochemical sensors [12,20]. Electrochemical methods have gained prominence in environmental applications for BTEX and its derivatives [3,24,25]. This is due to the advantages that the method offers such as rapid analysis, low cost, easy operation, high sensitivity, and good selectivity [26,27].

The literature reports an increasing in the application of reduced graphene oxide (rGO) as a modifier for electrode surfaces [28,29]. Graphene is a two-dimensional nanostructured material (carbon sheets) formed only by sp^2 type carbons (three planar orbitals and 120° connection angles). Graphene oxide (GO) is a graphene sheet with carboxylic groups at its edges and phenol hydroxyl, and epoxide groups on its basal plane [30]. Thermal or chemical reduction can decrease the concentration of functional groups in GO to produce rGO [31]. Therefore, the structure of graphene is composed of interconnected hexagons of carbon atoms and it is considered the strongest, thinnest material known to exist [32,33]. Among the most

diverse properties of this material, it is worth mentioning the high thermal conductivity, good charge carrier mobility, exclusive mechanical and electrical properties, and large specific surface area [33,34].

Based on these findings, the objective of this work is the development of a simple and sensitive method through the use of the electrochemical sensor GCE/rGO for the simultaneous analysis of BQ and RS in soil and groundwater samples, from a retail fuel station. In the literature there are several applications of electrochemical sensors modified with graphene [28,35–38], in special for the simultaneous determination of compounds derived from benzene such as catechol, hydroquinone (HQ) and RS [39–41], HQ and catechol [42–44]. However, so far of our knowledge, this is the first time that the sensor studied in this work is used to simultaneous detection of *p*-benzoquinone and resorcinol, fact that motivated this study.

2. MATERIALS AND METHODS

2.1. Reagents and Solutions

Chemical reagents were of analytical grade and used without further purification. Aqueous solutions were prepared with Milli-Q deionized water with resistivity ≥ 18 MΩ cm. Iron(II) chloride tetrahydrate, potassium sulfate, potassium ferricyanide, acetic acid, hydrogen peroxide, acetone, and resorcinol (purity ≥ 98%) were obtained from Merck Company. Graphite powder (particle size < 20 μm), sulfuric acid, potassium permanganate, hydrochloric acid, *p*-benzoquinone (purity ≥ 98%), and Nafion® were purchased from Sigma-Aldrich. Sodium acetate was obtained from Isofar, and hydrazine sulfate from CRQ Chemical. The stock solution of *p*-benzoquinone 4 mM was prepared by dissolving the mass of the reagent in a mixture of water and ethanol in the proportion of 1:1 (v/v) and the stock solution of resorcinol 4 mM was prepared in deionized water.

2.2. Apparatus

The electrochemical experiments were performed in a conventional three-electrode cell, in which GCE (geometric area = 0.0712 cm^2), $Ag|AgCl|KCl_{sat}$, and a platinum wire were respectively used as working, reference, and auxiliary electrodes. The measurements were performed on a Metrohm Autolab PGSTAT 302 potentiostat/galvanostat, controlled by NOVA 1.10 software. FTIR spectroscopic analyses were recorded with a Shimadzu IR Prestige-21 spectrometer in the 400 to 4000 cm^{-1} range.

2.3. Synthesis of Reduced Graphene Oxide (rGO)

Graphite oxide (GiO) was prepared following the method proposed by Hummers and Offeman [45]. For the synthesis of rGO 500 mg of GiO were dispersed in 170 mL of deionized water and sonicated for 2 h to exfoliate oxidized graphite particles to graphene oxide (GO)

sheets. Afterwards, hydrazine sulfate (450 mg) was added and this mixture remained under stirring at 80 °C for 24 h. The product obtained was filtered, and washed with 250 mL of deionized water and 100 mL of acetone. The material was dried at 40 °C for 12 h [46]. Subsequently, suspensions of 1 mL of rGO in methanol (3.0 g L^{-1}) containing different proportions (0.25, 0.5, 1.0, and 2.0 %) of Nafion® were prepared, which were sonicated for 30 min. A 5 µL aliquot of each suspension was then placed onto the GCE surface, then allowed to evaporate at room temperature, then another 5 µL were dripped, forming a film of total volume of 10 µL to leave a thin film of rGO immobilized onto the electrode surface.

2.4. Collection and Preparation of Sample

Soil, groundwater samples, and water samples from the water and oil separator box were collected in the monitoring wells of a fuel retail station situated in the city of São Luís-MA. Amber glass bottles were used to collect the samples. Before use, these containers were washed with water and common detergent and then placed in an Extran solution (5%, neutral) for 2 hours. The bottles were rinsed with ultrapure water and placed in a drying oven at 100 ºC for 24 hours. The collected samples were placed in an ice bath and transported directly to the laboratory where the analyses were performed. The samples remained stored at 4 °C and were used in the experiments within 20 days after collection. The water sample from the separator box was filtered with a 0.45 µm membrane filter, while the well water sample was not pretreated, before analysis. For the soil sample, 1.0 g was weighed and 4.0 mL of ultrapure water was added to it, after what the container was capped and allowed to decant for 2 h at room temperature. For the voltammetric analysis, 4.0 mL aliquots of the real samples were placed in the electrochemical cell, together with 6.0 mL of acetate support electrolyte, at pH 6.0.

2.5. Analytical Procedure

Voltammetric analysis was carried out using 0.1 M acetate solution (pH 6.0) as supporting electrolyte, and containing BQ and RS into the cell. Cyclic voltametric (CV) measurements were obtained in the potential range between −0.3 and 1.1 V for both analytes at a scan rate of 0.02 V s^{-1}. For SWV studies, the following parameters were used after optimization: frequency = 10 Hz, step potential = 2 mV s^{-1}, amplitude = 20 mV. The determination of the analytes was performed by the standard addition method. Electrochemical impedance spectroscopy (EIS) measurements were performed in 0.1 M KCl containing 5×10^{-3} M $K_3[Fe(CN)_6]/K_4[Fe(CN)_6]$ (1:1) by applying a sine wave with an amplitude of 0.01 V rms in the frequency range from 0.1 to 1×10^5 Hz at a potential of 0.21 V.

3. RESULTS AND DISCUSSION

3.1. Characterization of rGO

The GiO and rGO materials were characterized by FTIR, whose spectra are shown in Figure 1. The broad and intense band between 3640 cm^{-1} - 2400 cm^{-1} for GiO (red line) shows the presence of free hydroxyl groups (−OH) and intramolecular hydrogen bonding with C = O [47–49].

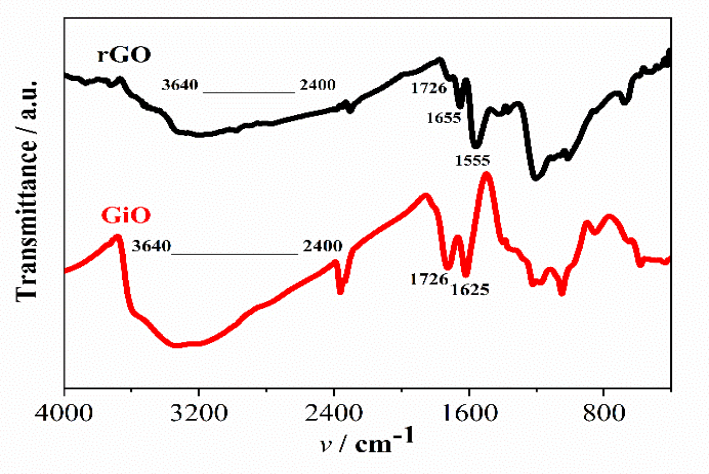

Figure 1. FTIR spectra of the GiO and rGO samples

This broadband also appears on the rGO spectrum (black line), but with less intensity, showing the partial removal of hydroxylated functional groups introduced in the graphite oxidation process. In other words, the decrease in the intensity of this band is an immediate consequence of the reduction process of GO to rGO.

The vibrational frequency at 1726 cm^{-1} in the GiO spectrum refers to the C=O stretch for aliphatic aldehydes of unbranched chains, in addition to the frequency in 1625 cm^{-1} associated with the C=O group with hydrogen bonds in enolic form [48]. These frequencies no longer appear on the rGO spectrum after the GO reduction process. The vibrational frequencies (of rGO) that appear around 1655 cm^{-1} and 1555 cm^{-1} are typical frequencies of nitrogen compounds. Although it is not possible to precisely determine only by FTIR to which group such frequencies refer, these frequencies support the claim that the reduction of GO in the presence of hydrazine sulfate introduces a series of nitrogenous groups in the rGO, such as amines, amides, nitriles, among others [48].

3.2. Electrochemical Behaviour of GCE/rGO, Mechanism, and Optimization of Experimental Parameters

The electrochemical response of BQ and RS on the GCE/rGO was evaluated by the CV technique (Figure 2) in the potential range of −0.3 to 1.1 V, in 0.1 M acetate electrolyte solution (pH 6.0) containing 3×10^{-3} M of each analyte.

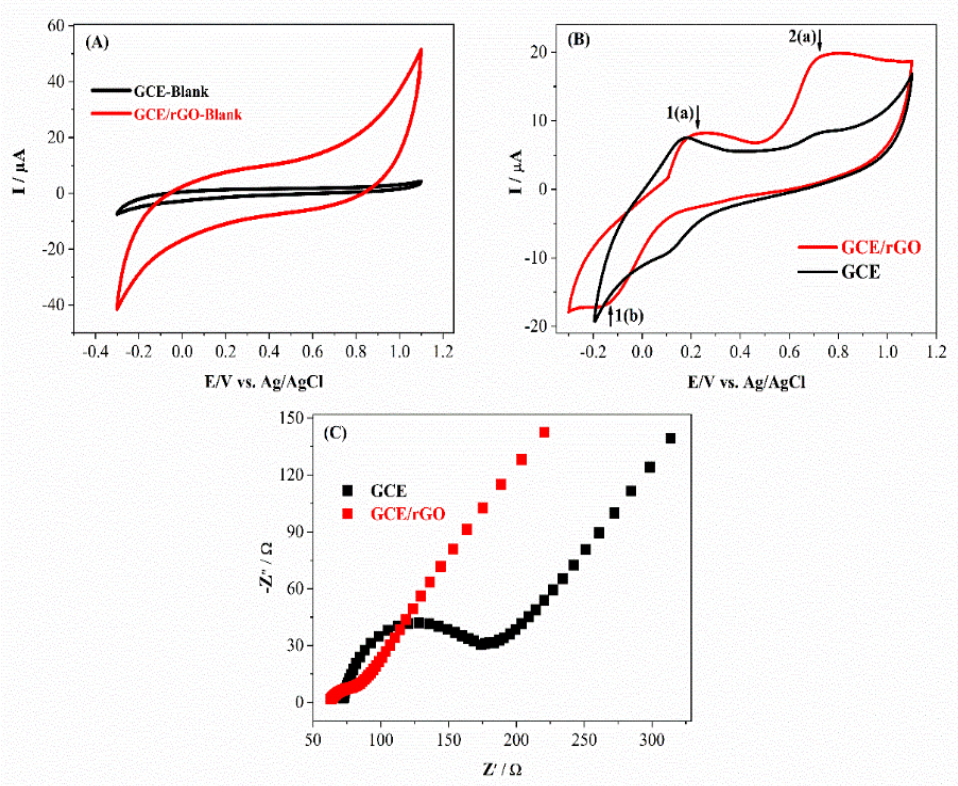

Figure 2. Cyclic voltammograms obtained for GCE and GCE/rGO in 0.1 M acetate electrolyte solution (pH 6.0) and scan rate of 20 mV s^{-1} in the absence (A) and in the presence of BQ and RS (3×10^{-3} M) (B). Nyquist plots obtained for GCE and GCE/rGO in 0.1 M KCl containing 5×10^{-3} M $K_3[Fe(CN)_6]/K_4[Fe(CN)_6]$ (1:1) at +0.21 V (C)

Figure 2A shows the cyclic voltammograms obtained in the 0.1 M acetate electrolyte solution for GCE and GCE/rGO, where no redox peaks were found in the applied potential range. As can be seen, there is only a greater residual current related to the GCE/rGO, indicating that the active surface area of the GCE/rGO is greater than that of the GCE.

Figure 2B shows the redox processes referring to the oxidation reactions (E_{ap} = 0.24 V) from HQ to BQ and the reduction (E_{pc} = −0.11 V) from BQ to HQ, irreversible oxidation of RS E_{ap} = 0.75 V.

The EIS study (Nyquist graphs) for GCE and GCE/rGO was performed in 0.1 M KCl solution, because the literature reports a better performance of the redox pair $K_3[Fe(CN)_6]/K_4[Fe(CN)_6]$ in neutral or near neutral conditions [50] as illustrated in Figure 2C. The linear part, in the low-frequency region, is attributed to the diffusion process [51]. The increase or decrease in the diameter of the semicircle is directly associated with the blocking behaviour of the electrode surface for the transfer of charge to the redox pair in the solution [52]. The analysis of Figure 2C suggests that the transfer of electrons to the surface of the GCE/rGO has a lower resistance in relation to the GCE, as it presents a smaller semicircle diameter (R_{ct} = 24 Ω) in relation to the GCE (R_{ct} = 110 Ω).

The oxidation of RS and BQ in GCE/rGO was investigated in different supporting electrolytes (acetate, Britton-Robinson, and phosphate buffers) all at a concentration of 0.1 M and pH 6.0, in the presence of 1.2×10^{-4} M of BQ and RS. The supporting electrolyte that presented the highest peak current for the two analytes was acetate (Figure not shown). Therefore, the acetate solution was chosen as supporting electrolyte for further studies.

Figure 3 shows the influence of pH on the voltammetric response to BQ and RS oxidation, in 0.1 M acetate electrolyte solution, [BQ] = [RS] = 1.2×10^{-4} M, in the 3.0 to 8.0 pH range using the SWV technique.

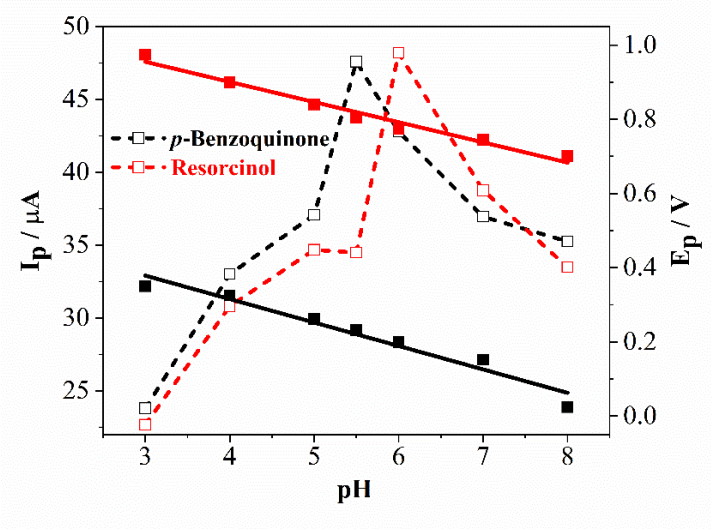

Figure 3. pH variation study carried out in 0.1 M acetate electrolyte solution, containing 1.2×10^{-4} M of BQ (black) and RS (red). Dashed line: Peak current response as a function of pH; Continuous line: Peak potential response as a function of pH

When the hydrogen concentration is varied the peak potential values and even change peak current magnitudes, depending on the type of redox system studied.

The results showed that the peak potential of BQ and RS shift to less positive potentials with the increase in the pH value. Such behaviour is expected for electroactive species that obey the Nernst equation [53]. The linear regression equations obtained were: E_p = 1.12 – 0.0543pH and E_p = 0.57 – 0.0632pH para BQ e RS, respectively.

The proton/electron ratios (H^+/e^-) calculated were 1.1 for BQ and 0.94 for RS, both of which are therefore close to 1, which indicates that protons and electrons participate equally in the redox reaction of BQ and RS.

The redox reversibility of the studied systems was evaluated (Figure 4). According to the literature [12,54–56] and as shown in Figure 4A the intensity of the peak current of BQ varied linearly with the square root of the frequency. In contrast, the RS response indicates an irreversible process (Figure 4B).

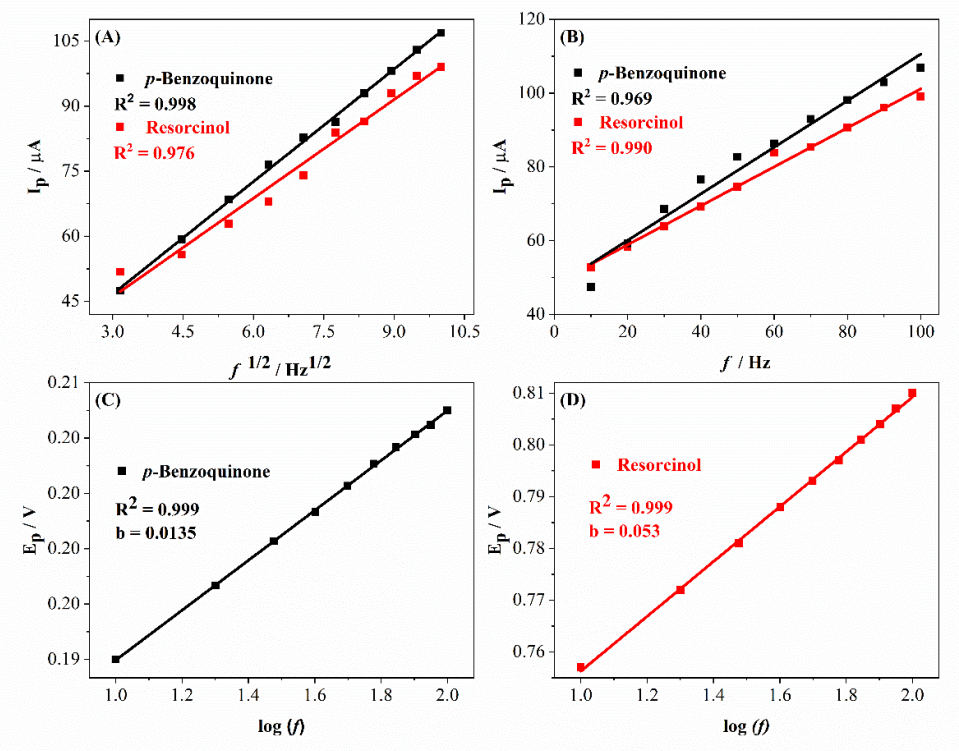

Figure 4. Peak current as a function of the square root of the frequency (A) and as a function of frequency (B) for BQ (black) and RS (red). Study of peak potential as a function of log frequency for BQ (C) and RS (D). Conditions: frequency: 10 Hz; ES: 0.1 M supporting electrolyte: acetate (pH: 6.0); amplitude: 20 mV; [BQ] = [RS] = 1.2×10^{-4} M.

As can be seen, the reversibility attributed to BQ should be justified by the physical adsorption of products and/or reagents on the electrode surface. For irreversible systems, the adsorptive process of the species is controlled and the peak current has a linear relationship with the frequency [55–57].

The relationship between peak potentials and frequency variation allows us to obtain information about the number of electrons involved in the redox process. For reversible systems, the model in equation 1 is applied, and for irreversible systems, the model in equation 2 is applied [53,57,58].

$$\frac{\Delta Ep}{\Delta \log(f)} = \frac{-2.3.R.T}{2nF} \quad (1)$$

$$\frac{\Delta Ep}{\Delta \log(f)} = \frac{-2.3.R.T}{\alpha nF} \quad (2)$$

F (J V^{-1} mol^{-1}) is the Faraday constant; R (J K^{-1} mol^{-1}) is the gas constant; T (K) is the system temperature; n is the number of electrons involved in the electrodic reaction and α (0.5) is the charge transfer coefficient. The linear relationships for BQ and RS (Figures 4C and 4D) presented slope coefficients for BQ (b = 0.015) and RS (b = 0.053). This implies that in each system, 2 electrons participate in the redox process.

Considering the present results, the following redox reactions were proposed following the literature [15,59,60], as illustrated in Figure 5.

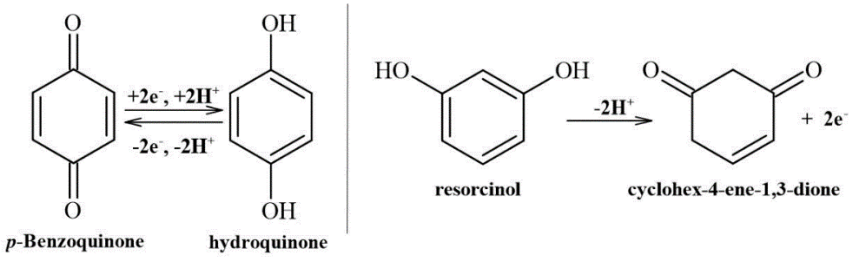

Figure 5. Redox reactions of *p*-benzoquinone and resorcinol

The oxidation reaction of RS considers the generation of a quinone, a product of considerable instability such as a polymeric film formed on the electrode surface. This film is thermodynamically stable in order to make the RS reduction process unfeasible. Therefore, no reduction peak is observed after the RS oxidation process [61,62].

In terms of optimization analytical, the main parameters were evaluated. The BQ showed the highest current at pH 5.5 and the second highest current at pH 6.0 (Figure 3), while RS showed the highest peak current at pH 6.0. Therefore, considering the simultaneous determination of analytes the pH 6.0 was the value chosen for further analysis.

The study of the variation in the frequency of application of the potential pulses was carried out between 10 and 100 Hz with the step potential equal to 2 mV and amplitude of 50 mV (Figure 4 B). This study showed that despite the highest current not being the one corresponding to 10 Hz, however, considering the simultaneous determination and the best voltammetric profile of BQ and for RS (figure not shown) the frequency of 10 Hz was chosen for further studies.

The amplitude effect was studied between 10 mV and 100 mV, with a frequency of 10 Hz, and a step potential of 2 mV (Figure 6A). The BQ showed the largest peak current in the amplitude of 100 mV. RS, on the other hand, exhibited an opposite behaviour, having its higher peak current in the amplitude of 20 mV and the lowest in 100 mV. This behaviour is in agreement with the literature, because for irreversible systems, the half-wave width remains constant for amplitudes greater than 20 mV [54,55]. Therefore, the 20 mV amplitude value was chosen for the simultaneous determination of the analytes. This behaviour is in accordance with the SWV theory for totally irreversible systems with the species adsorbed on the electrode surface [57,63]. The study of the relationship between amplitude and potential (see insertion of figure 6A), showed that the increase in amplitude caused a shift in the potentials of RS to less positive values, while for BQ, the potential remained practically constant. For irreversible systems, increasing the amplitude displaces the values of peak potentials. However, for reversible systems, increasing the amplitude practically does not displace the peak potential

[57,64]. Therefore, the study proves that the RS redox process is an irreversible system, while the BQ redox process is a reversible system.

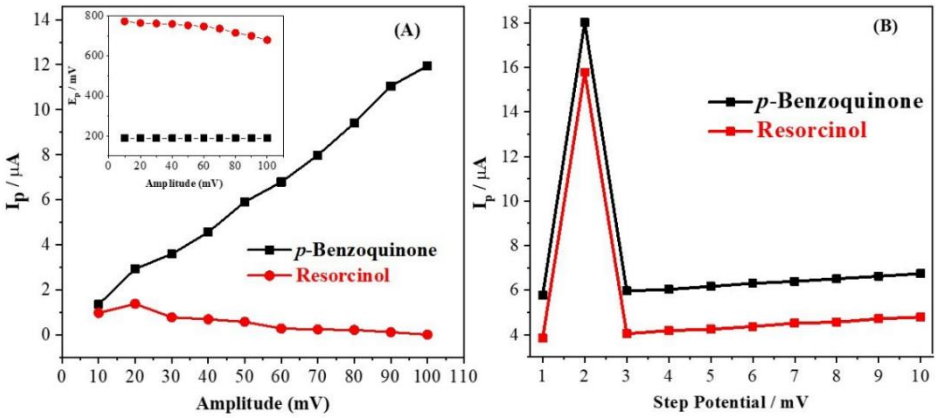

Figure 6. (A) Amplitude study performed (10 to 100 mV) BQ (black) and RS (red). Continuous line: I_p vs amplitude; Dashed line: E_p vs amplitude. (B) Peak current as a function of the step potential (1.0 to 10 mV). Conditions: frequency: 10 Hz; 0.1 M acetate electrolyte solution; pH: 6.0; amplitude: 20 mV; [BQ] = [RS] = 1.2×10^{-4} M

The study of step potential (Figure 6B) demonstrated that the best peak current for both analytes was in 2 mV. Therefore, it was chosen for the simultaneous study of compounds BQ and RS. Other parameters were also investigated.

The pre-concentration potential was varied from −0.35 to 0.0 V with the deposition time fixed at 30 s. The preconcentration time was varied from 10 to 90 s with the deposition potential fixed at 0.0 V. The best results found for these parameters were 0.0 V and 40 s, respectively. Table 1 presents all parameters optimized for the determinations of BQ and RS.

Table 1. Parameters evaluated and optimized for the simultaneous detection of BQ and RS by SWV technique

Parameters	**Studied interval**	**Value chosen**
Frequency (Hz)	10 – 100	10
Amplitude (mV)	10 – 100	20
Step Potential (mV)	1 – 10	2
Pre-concentration Potential (V)	−0.35 – 0.0	0.0
Pre-concentration Time (s)	10 – 90	40
Nafion® content (%)	0.25 – 2	0.5
Volume of rGO suspension (µL)	5 – 20	10

3.3. Analytical Performance and Interference Study

Figure 7 shows a typical response of the electrochemical sensor for simultaneous determination BQ and RS in an aqueous medium. To verify its performance and applicability, the sensor was evaluated for the analysis of BQ and RS in real water samples. These samples were determined to be free of BQ and RS by HPLC-MS/MS analysis and then spiked with known concentrations of the two analytes, thus maintaining the matrix effect on the obtained response. The internal graphs show the variation of the anodic peak current as a function of the analyte concentration.

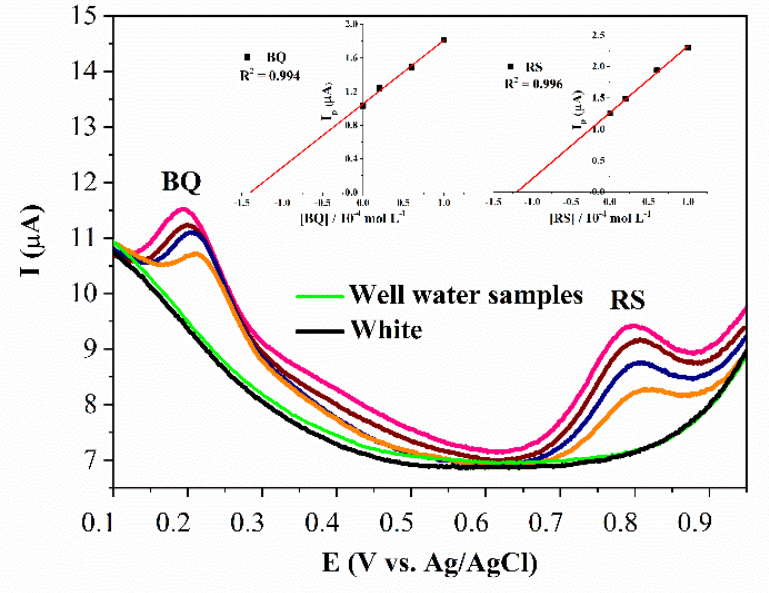

Figure 7. SWV with GCE/rGO, for detection of BQ and RS in real well water sample, in the concentration range: 20 to 100 μM in optimized conditions: supporting electrolyte: 0.1 M acetate electrolyte solution (pH = 6.0); frequency = 10 Hz, step potential = 2 mV s^{-1}, amplitude = 20 mV. Inserted figure (I_p vs. [BQ and RS])

Simultaneous analysis of BQ and RS with the GCE/rGO sensor was performed by SWV with analyte concentrations ranging from 20 to 100 μM. It was observed that the peak currents increased with increasing analyte concentrations. While the RS peak potentials remained unchanged, the BQ peak potentials shifted to less positive values; however, this fact did not caused any deviation from the linearity between the current and the analyte concentration, as shown in Figure 7 (inset). The equations obtained by linear regression of the analytical curves of BQ and RS were, respectively, $I_{ap}(\mu A) = 1.053 + 0.755[BQ]$ ($R^2 = 0.994$) and $I_{ap}(\mu A) = 1.265 + 1.0567$ [RS] ($R^2 = 0.996$).

The limits of detection (LOD) and quantification (LOQ) were calculated according to equations 3 and 4, respectively [55,56].

$$\mathrm{LOD} = \frac{3.\sigma}{s} \quad (3)$$

$$\mathrm{LOQ} = \frac{10.\sigma}{s} \quad (4)$$

Where: "σ" is the standard deviation of the mean of measurement of blanks (n = 10) in the potentials equivalent to those of the analyte peaks; "s" represents the slope obtained in the analytical curve.

The calculated LODs were, respectively, 0.37 μM and 0.81 μM for BQ and RS. The LOQ for BQ was 1.23 μM and for RS was 2.71 μM.

In the present work, the GCE/rGO presented LODs comparable to the other electrodes modified with graphene-based films. As can be seen, the found results are according to the literature (Table 2), emphasizing the relevance of the studied sensor.

Table 2. A comparison of the studied sensor with other found in the literature

Sensor	Analyte	Technique	Linear range (μM)	Slope (μA μM^{-1})	LOD (μM)	References
Bi_2WO_6/GCE[1]	RS	SWV	20-5000	654	4.3	[65]
p-rGO[2]	RS	DPV	5-90	-	2.62	[66]
ZnO/Co_3O_4 – MCPE[3]	RS	DPV	10-60	-	2.92	[15]
BDD[4]	BQ	DPV	18.1-925	5.67	24.74	[67]
MnO_2@Co-Ni MOFs/fMWCNTs/SPCE[5]	BQ	DPV	5-3×10^4	0.41	2.7	[68]
G-Cht[6]	RS	DPV	1-550	0.025	0.75	[69]
MWCNT/CoPc[7]	RS	SWV	0.99-8.3	17.10	0.42	[70]
GCE/rGO	RS	SWV	20-100	1.06	1.06	This work
GCE/rGO	BQ	SWV	20-100	0.75	0.75	This work

[1]Bi_2WO_6/GCE Bismuth tungstate nanocomposites and glassy carbon electrode
[2] p-rGO porous reduced graphene oxide
[3]ZnO/Co_3O_4 -MCPE[3] nanocomposite modified carbon paste electrode
[4]BDD Boron-doped Diamond
[5]MnO_2@Co-Ni MOFs/fMWCNTs/SPCE nanocomposite metal-organic frameworks functionalized multiwalled carbon nanotubes, screen printed carbon electrodes
[6]G-Cht graphene-chitosan composite film
[7] MWCNT/CoPc multiwalled carbon nanotubes cobalt phthalocyanine

The interference study was performed to assess the influence of one analyte on another and also considering other aromatic foreign species.

When relating the anodic peak currents of one analyte versus the concentration of the other analyte (Figures not shown), a linear relationship is verified for both analytes (BQ and RS) with $R^2 > 0.998$. This indicates that, for both systems, there is no interference in the oxidation process. It can be inferred that the studied sensor can be used for simultaneous analysis of BQ and RS.

The interference of other aromatic compounds can be seen in Table 3. In this study a mixed solution of BTEX and CC (containing equal parts of benzene, toluene, xylene, and catechol) was evaluated varying the concentration in the range of 20 to 120 µM, in the presence of 120 µM of BQ and RS.

Table 3. Interference percentage (%) of BTEX and CC in the peak current (I_p) of BQ and RS

I_p Analyte (µA)		**[BTEX and CC] (µM of each)**	**Interference (%)**	
BQ	RS		BQ	RS
8.99	3.84	0	0.00	0.00
8.99	3.84	20	0.00	0.00
9.01	3.71	40	0.22	3.40
9.32	3.58	60	3.67	6.77
9.66	3.31	80	7.45	13.80
9.43	3.12	100	4.89	18.75
9.52	3.09	120	5.89	19.53

%RSD (0.32 - 0.27)

As can be observed RS presented a higher interference index than BQ. This is justified by the fact that RS and CC are positional isomers. Therefore, up to the concentration of 120 µM of the BTEX and CC solution, there is no significant change in the peak currents of BQ and RS, evidencing the good selectivity of the sensor for BQ and RS in the presence of other compounds that contain an aromatic ring, including benzene derivatives.

Table 4 shows the results of the measurement repeatability study (ten scans) and repeatability in the preparation of the sensor or intermediate precision (also preparing six sensors on different days) for BQ and RS.

Table 4. Evaluation of GCE/rGO repeatability and intermediate precision

Repeatability	Average I (µA)	RSD (%)	Conc. (µM)
BQ	22.95	0.10	30
RS	18.17	0.36	20
Intermediate precision	Average I_p (µA)	RSD (%)	Conc. (µM)
BQ	22.77	0.12	30
RS	17.94	0.59	20

N1=10; N2=6

As can be seen in Table 4, there was no significant difference between the currents obtained for both BQ and RS. The studied sensor presented RSD<5%, which indicates good precision. It is noted, therefore, that the GCE/rGO has good repeatability of measurements and also good repeatability of sensor preparation, indicating that the GCE/rGO has high precision.

3.4. Application to Real Samples

The accuracy was evaluated through a recovery test, calculated using equation 5, that consists of the relationship between the concentration found and the added concentration [71]:

$$\%\, recovered = \frac{[found]}{[added]} \quad (5)$$

The recovery studies in real samples of soil, well water and water sample from separator box (Table 5) were carried out through the application of the optimized procedure.

Table 5. Recovery data regarding the simultaneous determination of BQ and RS in real samples

		Added (µM)		**Found (µM)**		**Recovery (%)**	
	Samples	BQ	RS	BQ	RS	BQ	RS
Soil[a]	1	20.0	20.0	19.5	20.0	97.5	100.0
	2	40.0	40.0	39.9	39.7	99.7	99.2
	3	60.0	60.0	61.8	60.0	103.0	100.0
Fuel Station Well Water[b]	1	20.0	20.0	20.0	20.0	100.0	100.0
	2	40.0	40.0	41.0	40.0	102.5	100.0
	3	60.0	60.0	60.0	57.3	100.0	95.5
	4	80.0	80.0	81.3	81.0	101.0	101.2
	5	100.0	100.0	97.0	99.0	97.0	99.0
Separator Box Water[c]	1	20.0	20.0	19.7	19.5	98.5	97.5
	2	40.0	40.0	40.5	41.0	101.2	102.5
	3	60.0	60.0	59.8	60.0	99.6	100.0
	4	80.0	80.0	80.0	80.0	100.0	100.0
	5	100.0	100.0	100.0	100.0	100.0	100.0

[a]%RSD (0.46 – 2.1); [b]%RSD (2.01 – 2.17); [c]%RSD (0.97 – 1.76)

4. CONCLUSION

A simple electroanalytical procedure was developed using the electrochemical sensor GCE/rGO, with important results on the redox processes of BQ and RS. The study of the electrochemical behaviour indicated an adequate electroanalytical response for the simultaneous determination of BQ and RS.

The GCE/rGO exhibited a linear behaviour with increasing concentration of BQ and RS, presenting low detection limits when compared with others from the literature for both analytes, being considered satisfactory for analytical application. Considering the simplicity, low cost, good selectivity, and precision, the proposed procedure can be seen as a viable alternative for the simultaneous determination of BQ and RS in real soil samples and groundwater.

Acknowledgments

The authors are grateful to CAPES/PROCAD-AM 2018 – Line 2; Number SCBA: 88887.200615/2018-00), CNPq (PQ 2017, Proc. 310664/2017-9), FAPEMA (Proc. Edital UNIVER-SAL-01136/17) and ANP (Research Project PMQC/QUALIPETRO, No 1.028/2021-ANP- PMQC), Research Project QUALIPETRO CONSEPE-UFMA N° 2.460/22], for the financial support and fellowships received.

Declarations of interest

The authors declare no conflicts of interest.

REFERENCES

[1] S. Adipah, J. Environ. Sci. Public Health 3 (2019) 1.
[2] G. Qu, G. Liu, C. Zhao, Z. Yuan, Y. Yang, and K. Xiang, Environ. Sci. Pollut. Res. 31 (2024) 1.
[3] I.C.B. Alves, J.R.N. Santos, E.P. Marques, L.C.M. Azevedo, M.A. Beluomini, N.R. Stradiotto, and A.L.B. Marques, Electroanalysis 36 (2024) e202300260.
[4] H. Anjum, K. Johari, N. Gnanasundaram, M. Ganesapillai, A. Arunagiri, I. Regupathi, and M. Thanabalan, J. Mol. Liq. 277 (2019) 1005.
[5] K. Šimkovič, and J. Derco, Monatsh. Chem. 150 (2019) 1869.
[6] L. Falzone, A. Marconi, C. Loreto, S. Franco, D.A. Spandidos, and M. Libra, Mol. Med. Rep. 14 (2016) 4467.
[7] M. Hadei, P.K. Hopke, M. Rafiee, N. Rastkari, M. Yarahmadi, M. Kermani, and A. Shahsavani, Environ. Sci. Pollut. Res. 25 (2018) 27423.
[8] F.A. Kuranchie, P.N. Angnunavuri, F. Attiogbe, and E.N. Nerquaye-Tetteh, Cogent Environ. Sci. 5 (2019) 1603418.
[9] E.T. Sousa, W.A. Lopes, and J.B. Andrade, Quim. Nova 39 (2016) 486.
[10] E. do Vale-Júnior, A.J. dos Santos, D.R. da Silva, A.S. Fajardo, and C.A. Martínez-Huitle, ChemElectroChem 6 (2019) 4383.
[11] O. Turkay, S. Barisci, H. Öztürk, B. Öztürk, and M.G. Şeker, J. Environ. Eng. 144 (2018) 04018124.
[12] S. Agrahari, A.K. Singh, R.K. Gautam, and I. Tiwari, Chemosphere 342 (2023) 140078.
[13] A. Dabhade, S. Jayaraman, and B. Paramasivan, Prep. Biochem. Biotechnol. 50 (2020) 849.
[14] U. Priyanka, and P.N.L. Lens, Microb. Technol. 157 (2022) 110020.
[15] S.B. Arpitha, B.E. Kumara Swamy, and J.K. Shashikumara, Inorg. Chem. Commun. 152 (2023) 110656.

[16] K.P. Moulya, J.G. Manjunatha, T.M. Almutairi, M. Nagaraja, and B. Somashekara, Monatsh. Chem. (2024) 1.
[17] D.J. DiScenza, L.E. Intravaia, A. Healy, S.B. Dubrawski, and M. Levine, Chemosensors 7 (2019) 5.
[18] T. Sun, H. Song, X. Xie, M. Sun, Y. Su, and Y. Lv, Chem. Eng. J. 470 (2023) 144029.
[19] S. Khan, D. Newport, and S. Le Calvé, Spectrochim. Acta. A. Mol. Biomol. Spectrosc. 243 (2020).
[20] J. Fabri, L.R.G. Silva, J.S. Stefano, J.F.S. Pereira, D.R. Cocco, R.A.A. Muñoz, and D.P. Rocha, Microchem. J. 191 (2023) 108810.
[21] M. Pastor-Belda, P. Viñas, N. Campillo, M. Hernández-Córdoba, and M. Hernández-Córdoba, Microchem. J. 145 (2019) 406.
[22] N.G. Davey, R.J. Bell, C.G. Gill, and E.T. Krogh, Atmos. Pollut. Res. 11 (2020) 545.
[23] Y. Liu, N. He, Y. Lu, W. Li, X. He, Z. Li, and Z. Chen, J. Pharm. Anal. 13 (2023) 209.
[24] R.B.S. Sawczuk, H.A. Pinheiro, J.N.R. Santos, I.C.B. Alves, H.D.C. Viegas, C.A. Lacerda, J.C.K. Sousa, E.P. Marques, and A.L.B. Marques, Int. J. Environ. Anal. Chem. 103 (2021).
[25] G. Qu, G. Liu, C. Zhao, Z. Yuan, Y. Yang, and K. Xiang, Environ. Sci. Pollut. Res. 31 (2024) 23334.
[26] Y.Y. Lei, X. Zhan, Y.W. Wu, and X.X. Yu, Talanta 268 (2024) 125287.
[27] B. Han, T.H. Rupam, A. Chakraborty, and B.B. Saha, Renewable Sustainable Energy Rev. 196 (2024) 114365.
[28] C. Zhang, J. Ping, and Y. Ying, Sci. Total Environ. 714 (2020).
[29] M.L. Báez, A. García, I. Martínez, C. González, M. Gómez, and B. Rodríguez, Int. J. Electrochem. Sci. 19 (2024) 100538.
[30] M.D. Budimir, and J.R. Prekodravac, Zero-Dimensional Carbon Nanomaterials (2024) 291.
[31] S. Kumuda, U. Gandhi, U. Mangalanathan, and K. Rajanna, J. Mater. Sci.: Mater. Electron. 35 (2024) 1.
[32] M.U. Arshad, C. Wei, Y. Li, J. Li, M. Khakzad, C. Guo, C. Wu, and M. Naraghi, Carbon 204 (2023) 162.
[33] N. Devi, R. Kumar, S. Singh, and R.K. Singh, Crit. Rev. Solid State Mater. Sci. 49 (2024) 72.
[34] S. Radhakrishnan, P.P. Das, A. Alam, S.P. Dwivedi, and V. Chaudhary, Proc. Inst. Mech. Eng. Part C. (2024).
[35] A.N. Brezolin, J. Martinazzo, J. Steffens, and C. Steffens, Sens. Actuators B Chem. 305 (2020) 127426.

[36] H. Silah, C. Erkmen, D. Nur Unal, and B. Uslu, Chapter 13-Sensing of Deadly Toxic Chemical Warfare Agents, Nerve Agent Simulants, and their Toxicological Aspects (2023) 297.
[37] H. Karimi-Maleh, R. Darabi, F. Karimi, C. Karaman, S.A. Shahidi, N. Zare, M. Baghayeri, L. Fu, S. Rostamnia, J. Rouhi, and S. Rajendran, Environ. Res. 222 (2023) 115338.
[38] Y.O. Donar, S. Bilge, D. Bayramoğlu, B. Özoylumlu, S. Ergenekon, and A. Sınağ, Trends Environ. Anal. Chem. 41 (2024) e00223.
[39] L. Huang, Y. Cao, and D. Diao, Sens. Actuators B 305 (2020) 127495.
[40] S. Yang, M. Yang, Q. Liu, X. Wang, H. Fa, Y. Wang, and C. Hou, J. Electrochem. Soc. 166 (2019) B547.
[41] Z.C. Fan, Z. Li, X.Y. Wei, Q.Q. Kong, J. Zhao, L. Li, J.H. Li, Z.Q. Liu, and Z.M. Zong, Microchem. J. 189 (2023) 108543.
[42] Y. Xue, M. Noroozifar, R.M.A. Sullan, and K. Kerman, Chemosphere 342 (2023) 140003.
[43] Y.M. Ahmed, M.A. Eldin, A. Galal, and N.F. Atta, Sci. Rep. 14 (2024) 1.
[44] Q.Q. Xu, Q.Q. Wang, Z.G. Liu, Z. Guo, and X.J. Huang, ACS Sustain. Chem. Eng. 11 (2023) 16764.
[45] W.S. Hummers, and R.E. Offeman, J. Am. Chem. Soc. 80 (1958) 1339.
[46] M. Roteta, R. Fernández-Martínez, M. Mejuto, and I. Rucandio. Appl. Radiat. Isot. 109 (2016) 217.
[47] W.A. Osunniran, J.A. Obaleye, A.C. Tella, and S.A. Amolegbe, Orbital: Electron. J. Chem. 10 (2018) 367.
[48] M.M.A. El-Sukkary, N.A. Syed, I. Aiad, and W.I. El-Azab, J. Surfactants Deterg. 11 (2008) 129.
[49] D.L. Pavia, G.M. Lampman, G.S. Kriz, and J.R. Vyvyan, Introduction to spectroscopy, Cengage Learning, Boston (2015).
[50] R. Sundaresan, V. Mariyappan, T.W. Chen, S.M. Chen, M. Akilarasan, M.A. Alsaigh, M. A. Ali, M.S. Elshikh, and J. Yu, Mater. Today Chem. 30 (2023) 101602.
[51] V. Chellappa, J. Annaraj, and S. Suresh, Mater. Chem. Phys. 319 (2024) 129330.
[52] B. Parasuraman, P. Shanmugam, S. Sangaraju, H. Rangaraju, D.R. Alphonse, M.N. Husain, and P. Thangavelu, Environ. Sci.: Adv. 3 (2024) 925.
[53] A. Bard, L. Faulkner, and H. White, Electrochemical methods: fundamentals and applications. John Wiley & Sons (2022).
[54] T. Thenrajan, M. Madhumalar, S. Kumaravel, R. Rajaram, S. Kundu, and J. Wilson, Mater. Adv. 5 (2024) 1691.
[55] A. Kassa, Z. Bitew, and A. Abebe, Sens. Biosensing. Res. 39 (2023) 100554.
[56] Y. Guo, and D. He, J. Mol. Liq. 385 (2023) 122242.

[57] M.F. Cabral, D. De Souza, C.R. Alves, and S.A.S. Machado, Ecletica Quim. 28 (2003) 41.
[58] D. De Souza, S.A.S. Machado, and L.A. Avaca, Quim. Nova 26 (2003) 81.
[59] M. Khodari, G.A.M. Mersal, E.M. Rabie, and H.F. Assaf, Int. J. Electrochem. Sci. 13 (2018) 3460.
[60] A.R.L. da Silva, A.J. Dos Santos, and C.A. Martínez-Huitle. RSC Advances 8 (2018) 3483.
[61] T. Iftikhar, M. Asif, A. Aziz, G. Ashraf, S. Jun, G. Li, and H. Liu, Trends Environ. Anal. Chem. 31 (2021) e00138.
[62] L. Baldino, L. Malfatti, G.B. Veselov, and A.A. Vedyagin, Materials 16 (2023) 6566.
[63] V. Pedrosa, L. Codognoto, and L.A. Avaca, Quim. Nova 26 (2003) 844.
[64] L.A. Currie, Anal. Chim. Acta 391 (1999) 103.
[65] T. Thenrajan, M. Madhu malar, S. Kumaravel, R. Rajaram, S. Kundu, and J. Wilson, Mater. Adv. 5 (2024) 1691.
[66] H. Zhang, X. Bo, and L. Guo, Sens. Actuators B Chem. 220 (2015) 919.
[67] E. Do Vale-Júnior, A.J. Santos, D.R. Silva, A.S. Fajardo, ChemElectroChem 6 (2019) 4383.
[68] S. Agrahari, A.K. Singh, R.K. Gautam, and I. Tiwari, Chemosphere 342 (2023) 140078.
[69] H. Yin, Q. Zhang, Y. Zhou, Q. Ma, T. Liu, L. Zhu, and S. Ai, Electrochim. Acta 56 (2011) 2748.
[70] I. Cesarino, F.C. Moraes, T.C. Ferreira, M.R. Lanza, and S.A. Machado, J. Electroanal. Chem. 672 (2012) 34.
[71] INMETRO (2010) DOQ-CGCRE-008.